Photochemical & Photobiological Sciences

PAPER

Cite this: *Photochem. Photobiol. Sci.*, 2019, **18**, 1197

Competing photochemical reactions of bis-naphthols and their photoinduced antiproliferative activity†

Matija Sambol,‡[a] Katja Ester,*[b] Stephan Landgraf,[c] Branka Mihaljević,[d] Mario Cindrić,[b] Marijeta Kralj[b] and Nikola Basarić*[a]

Received 20th November 2018,
Accepted 18th February 2019

DOI: 10.1039/c8pp00532j

rsc.li/pps

The photophysical properties and photochemical reactivities of a series of bis-naphthols **4a–4e** and bis-anthrols **5a** and **5e** were investigated by preparative irradiation in CH_3OH, fluorescence spectroscopy and laser flash photolysis (LFP). Methanolysis taking place *via* photodehydration (bis-naphthols: Φ_R = 0.04–0.05) is in competition with symmetry breaking charge separation (SB-CS). The SB-CS gave rise to radical ions that were detected for **4a** and **4e** by LFP. Photodehydration gave quinone methides (QMs) that were also detected by LFP (λ_{max} = 350 nm, $\tau \approx 1$–2 ms). In the aqueous solvent, excited state proton transfer (ESPT) competes with the abovementioned processes, giving rise to naphtholates, but the process is inefficient and can only be observed in the buffered aqueous solution at pH > 7. Since the dehydration of bis-naphthols delivers QMs, their potential antiproliferative activity was investigated by an MTT test on three human cancer cell lines (NCI-H1299, lung carcinoma; MCF-7, breast adenocarcinoma; and SUM159, pleomorphic breast carcinoma). Cells were treated with **4** or **5** with or without irradiation (350 nm). An enhancement of the activity (up to 10-fold) was observed upon irradiation, which may be associated with QM formation. However, these QMs do not cross-link DNA. The activity is most likely associated with the alkylation of proteins present in the cell cytoplasm, as evidenced by photoinduced alkylation of bovine and human serum albumins by **4a**.

Introduction

Quinone methides (QMs) are important intermediates in the chemistry and photochemistry of phenols.[1] The interest in the chemistry of QMs was primarily initiated owing to their biological activity,[2,3] and there is growing interest in the applications of QMs in organic syntheses.[4–8] It has been demonstrated that QMs react with amino acids,[9] proteins,[10] and nucleosides[11–14] and induce alkylation of DNA.[15–18] Furthermore, Freccero *et al.* demonstrated the ability of QMs to alkylate the G4 regions of DNA,[19–21] whereas Rokita *et al.* used the reversible alkylation ability of QMs leading to "immortalization of QM" by DNA as a nucleophile[22–24] potentially leading to a number of biomedical applications.[25] In particular, the cross-linking of DNA by metabolically formed QMs is linked to the mechanism of anticancer activity of some antibiotics such as mitomycin.[26–28]

QMs are reactive species that mostly have to be generated *in situ* since they have short lifetimes ranging from nanoseconds to seconds. Photochemical reactions represent mild methods for their generation, particularly in biological systems when spatial and temporal control is required.[29,30] The most commonly employed photochemical method is photodeamination of suitably substituted phenols.[9,31,32] However, photodehydration of hydroxybenzyl alcohols,[33,34] although taking place with a lower quantum yield than deamination, is even more appealing since the hydration of photochemically generated QMs regenerates the active species. An on-going study in our group involves the generation of QMs by photodehydration from suitable precursors, and investigation of their biological effects.[35–38] Recently we have demonstrated

[a]*Department of Organic Chemistry and Biochemistry, Ruđer Bošković Institute, Bijenička cesta 54, 10 000 Zagreb, Croatia. E-mail: nbasaric@irb.hr; Fax: +3851 4680 195*
[b]*Division of Molecular Medicine, Ruđer Bošković Institute, Bijenička cesta 54, 10 000 Zagreb, Croatia. E-mail: kester@irb.hr; Fax: +3851 4561 010*
[c]*Institute of Physical and Theoretical Chemistry, Graz University of Technology, Stremayrgasse 9, A-8010 Graz, Austria*
[d]*Division of Materials Chemistry, Ruđer Bošković Institute, Zagreb, Croatia*

†Electronic supplementary information (ESI) available: Synthetic procedures, fluorescence and LFP data, noncovalent binding to albumins, mass spectra measured by MALDI-TOF/TOF of BSA and HSA after photochemical alkylation, DNA cross-linking and antiproliferative data, ^{1}H and ^{13}C NMR spectra for all new compounds. See DOI: 10.1039/c8pp00532j

‡Current address: Fidelta Ltd, Prilaz baruna Filipovića 29, 10000 Zagreb, Croatia.

that photogenerated **QM1** formed from anthrol **1** exhibits higher cytotoxicity on cancer stem cell lines than on normal cancer cells.[39] However, monofunctional QM formed from **1** could only alkylate biological molecules. To enhance the biological activity of QMs our next idea was to prepare bi-functional molecules that could induce cross-linking. Therefore, we designed bis-phenol molecules **2** (Fig. 1) and investigated their biological effects upon F^- induced QM formation.[40] That is, DNA cross-linking by bi-functional molecules is known to be the most cytotoxic event leading to cell death.[41] Unfortunately, bis-phenols did not cross-link DNA and did not exhibit antiproliferative activity with or without the treatment with F^-, and the lack of the effect was connected with the inability to form bi-functional **QM2**. Instead of **QM2** formation, faster hydrolysis of QM took place leading to the destruction of the active molecules.

Herein we report an investigation of the photochemical generation of bi-functional QMs, which are derived from naphthol **3**[42] and anthrol **1** QM precursors,[39] and are anticipated to cross-link DNA (Fig. 2). The main advantage compared to bis-phenols **2** is the fact that hydration of the corresponding QMs regenerates the precursor molecules enabling re-photoactivation and re-generation of QMs. Investigation of the photochemical reactivity of **4** and **5** was particularly interesting in view of the recent findings by Vauthey *et al.* that bichromophoric systems in polar solvents undergo symmetry breaking charge separation (SB-CS).[43] Thus, we report on the competition among SB-CS, photodehydration and excited state proton transfer (ESPT). The photochemical reactivity was investigated by preparative irradiation and the photophysical properties of the molecules by fluorescence spectroscopy. Formation of reactive intermediates was probed by laser flash photolysis (LFP). Our main finding is that photodehydration, which is an ultrafast reaction,[34] competes well with the SB-CS, but the ESPT is significantly hampered. Furthermore, the antiproliferative activity of **4** and **5** was investigated *in vitro* against three human cancer cell lines NCI-H1299 (lung carcinoma), MCF-7 (breast adenocarcinoma) and SUM159 (pleomorphic breast carcinoma), combined with irradiation. Enhanced antiproliferative activity was ascribed to the intracellular formation of QMs that however do not cross-link DNA, but induce alkylation of proteins.

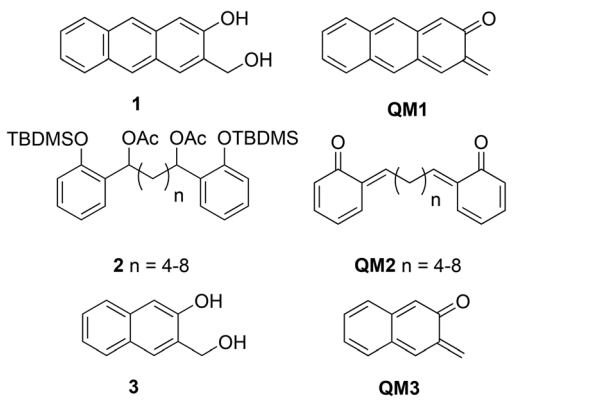

Fig. 1 Precursors for the QM generation from a literature precedent.

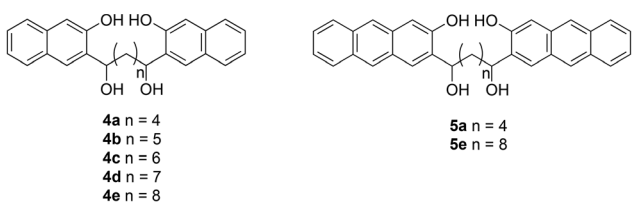

Fig. 2 Structures of bifunctional QM precursors.

Results and discussion

Synthesis

Synthesis of bis-QM precursors was based on the one pot double Grignard reaction with an appropriately protected carbaldehyde, as recently described for bis-phenols.[40] Thus, bis-naphthols were prepared from TBDMS-protected aldehyde **6** giving TBDMS-protected naphthols **7** as a mixture of diastereomers that were transformed to diastereomeric bis-naphthols **4** (Scheme 1).

Synthesis of bis-anthrols **5** followed the same strategy as described for bis-naphthols, by the double Grignard reaction of TBDMS-protected anthrol carbaldehyde **8**, and subsequent F^- induced silyl deprotection from the TBS-protected bis-anthrols **9**. However, bis-anthrols **5** were obtained in lower yields then bis-naphthols, and many problems were encountered during their purification due to their low solubility in most solvents. Therefore, only two derivatives **5** were prepared.

Photomethanolysis

Irradiation of bis-naphthols **4** or bis-anthrols **5** in the presence of CH_3OH is expected to give rise to photomethanolysis *via* QM intermediates.[38,42] Therefore, to show that **4** and **5** undergo photodehydration, we first performed preparative irradiation of selected bis-naphthols **4a**, **4b** and **4e**. After 1 h irradiation (20 mg, 10 × 8 W, 300 nm) in CH_3OH–H_2O (4 : 1), the conversion to products was >95%, whereupon mono- and bis-adducts **10** and **11** were formed, which were isolated by HPLC and characterized by NMR (Scheme 2).

The efficiency of the photomethanolysis for all bis-naphthols was measured by using a KI/KIO_3 actinometer (Φ_{254} = 0.74).[44,45] Irradiation was performed with monochromatic light at 254 nm in CH_3OH–H_2O (4 : 1), and the composition of the irradiated solution was analyzed by HPLC and UPLC/MS. The UPLC/MS analysis after photolysis showed the presence of molecular ions for reactants **4**, and photomethanolysis products **10** only, particularly important for molecules **4c** and **4d** whose preparative photolysis were not conducted. In addition to bis-naphthols **4**, the quantum yield for the photomethanolysis was measured for 3-hydroxymethyl-2-naphthol (**3**). Similar quantum yields for photomethanolysis were obtained for all derivatives **4**, as well as for **3** (Table 1). The

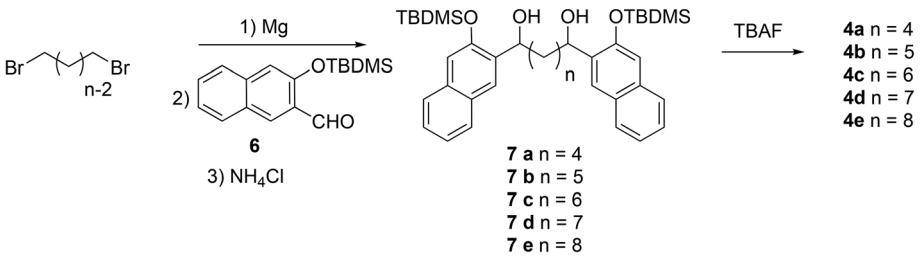

Scheme 1 Synthesis of bis-naphthol QM precursors.

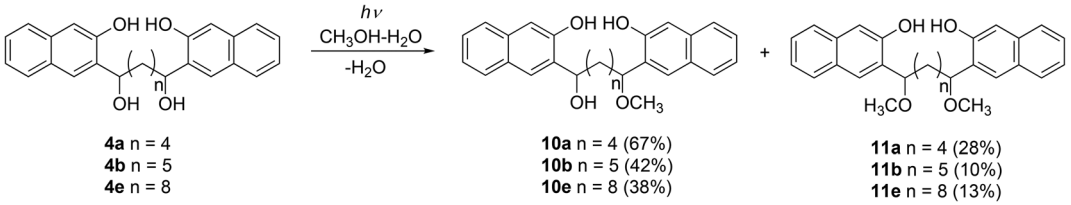

Scheme 2 Photomethanolysis of bis-naphthols **4**.

Table 1 Quantum yields of photomethanolysis (Φ_R) of **4**[a]

Comp.	Φ_R
4a	0.05 ± 0.01
4b	0.05 ± 0.01
4c	0.04 ± 0.01
4d	0.04 ± 0.01
4e	0.04 ± 0.01
3	0.04 ± 0.01[b]

[a] Determined by using the KI/KIO_3 actinometer (Φ_{254} = 0.74).[44,45] Irradiation performed in CH_3OH–H_2O (4 : 1). The measurement was performed in triplicate and the average value is reported. The quoted error corresponds to the standard deviation. [b] The quantum yield for the photoelimination of ethanol from 3-ethoxymethyl-2-naphthol is Φ = 0.17.[42]

result indicates that additional naphthol chromophores in molecules **4** do not affect the naphthol photoreactivity in the dehydration, and suggests that the photomethanolysis takes place *via* the same reaction mechanism as reported for the monochromophoric molecule **3**,[42] *via* a QM intermediate.

Due to the very low solubility of anthrols **5** in most common organic solvents except DMSO, the irradiation of **5a** and **5e** was performed in 1% DMSO/CH_3OH. After 10 min irradiation (1 mg, 1 × 8 W, 350 nm), the conversion to products was 70% and 40%, respectively. Due to problems with solubility, photochemical reactions on a larger scale and chromatographic separations to isolate products were not conducted. Instead, ether **13e** was prepared by a thermal acid-catalyzed methanolysis (see the Experimental section) and used for characterization. UPLC-MS analysis of **13e**, and a comparison with the irradiated mixtures indicated that ethers were formed in the photochemical reaction. Products **12** and **13** were formed in the total 5% yield from **5a** and the total 10% yield from **5e** (Scheme 3). In addition, irradiation gave a complex mixture of unidentified products in 65% yield from **5a** and 30% yield from **5e**. Since the photomethanolysis reactions were not clean, the reaction quantum yields for bis-anthrols **5** were not measured.

Absorption and fluorescence measurements

Photodehydration of naphthols is known to take place *via* a singlet excited state.[37,42] To obtain more information on the singlet excited state properties of bis-naphthols, and their reactivities, we performed absorption and fluorescence measurements (for all absorption and fluorescence spectra see Fig. S1–S13 in the ESI†). Due to their low solubility, spectroscopic investigation of anthrols **5** was not conducted. The absorption spectra of bis-naphthols are characterized by three absorption bands, at ≈220, 270 and 330 nm, the typical pattern for 2-naphthol (Fig. 3). Regardless of the alkyl spacer chain length

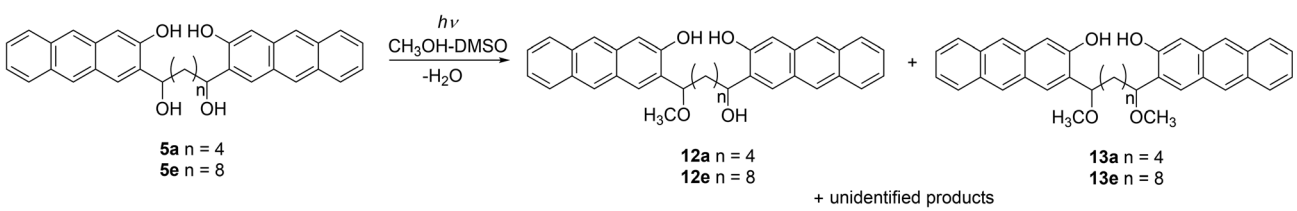

Scheme 3 Photomethanolysis of bis-anthrols **5**.

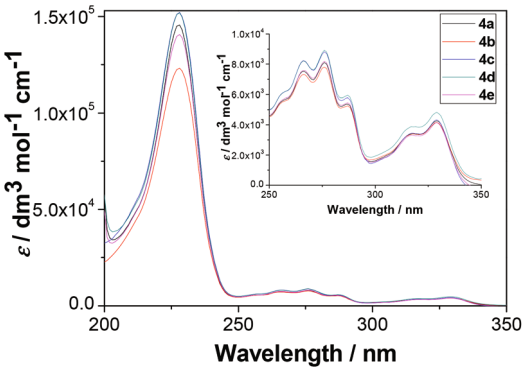

Fig. 3 Absorption spectra of bis-naphthols **4** in $CH_3OH–H_2O$ (4 : 1).

the compounds have similar absorptivities, which is about double compared to 3-hydroxymethyl-2-naphthol (**3**, see Fig. S11 in the ESI†). The finding suggests that two chromophores do not interact intramolecularly in the ground state.

Fluorescence spectra were recorded in CH_3CN and $CH_3CN–H_2O$ (Fig. 4), where differences were anticipated due to excited state proton transfer (ESPT) pathways,[46] which are only possible in the presence of proton accepting solvents.[47–50] That is, 2-naphthol is a well-known example of a photoacid that exhibits dual fluorescence due to emission from the naphthol and naphtholate.[51] Interestingly, the fluorescence spectra for bis-

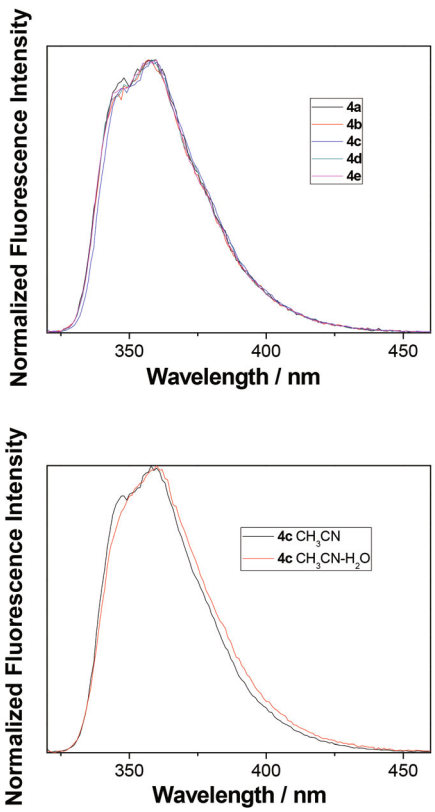

Fig. 4 Normalized fluorescence spectra (λ_{ex} = 310 nm) of bis-naphthols **4** in CH_3CN (top) and **4c** in CH_3CN and $CH_3CN–H_2O$ (3 : 1) (bottom).

Table 2 Fluorescence quantum yields for bis-naphthols **4** in CH_3CN and $CH_3CN–H_2O$ (3 : 1)[a]

	Φ_f (CH_3CN)	Φ_f ($CH_3CN–H_2O$)
4a	0.27 ± 0.03	0.27 ± 0.03
4b	0.24 ± 0.03	0.26 ± 0.02
4c	0.22 ± 0.03	0.25 ± 0.02
4d	0.25 ± 0.03	0.27 ± 0.03
4e	0.24 ± 0.02	0.25 ± 0.02

[a] Measured by using quinine sulfate in 1.0 N H_2SO_4 (Φ_f = 0.546).[52] One fluorescence measurement was performed by exciting the sample at three different wavelengths (300, 310 and 320 nm), and the average value was calculated. The quoted error corresponds to the standard deviation.

naphthols **4** did not differ in these two solvents suggesting that bis-naphthols do not undergo ESPT. Furthermore, the fluorescence quantum yields (Φ_f) were measured in CH_3CN and $CH_3CN–H_2O$ (Table 2) by using quinine sulfate in 1.0 N H_2SO_4 (Φ_f = 0.546).[52] The same values of Φ_f in both solvents indicate that the ESPT nonradiative deactivation pathway from S_1 in the protic solvent for **4** does not exist or is very inefficient, in contrast to the typical photophysics of simple naphthols.

Prompted by the non-observation of the naphtholate emission from **4** in the aqueous solvent, we investigated the effect of pH on the fluorescence properties of **4a**. The spectra were recorded in $CH_3CN–H_2O$ (1 : 1) without buffer and in the presence of sodium phosphate buffer (0.05 M) at different pH values (Fig. 5). Upon addition of the buffer, at pH values >6.9 we detected a shoulder in the spectrum at ≈430 nm that can be assigned to the naphtholate emission. Indeed, upon further addition of a base (at pH > 9.5), the typical dual emission of the naphthol and naphtholate can be seen (see Fig. S13 in the ESI†). Attempts to process the fluorescence data by nonlinear regression analysis and calculate the pK_a^* failed due to too small changes in the fluorescence spectra in the near-neutral region. However, from the maxima of the emission of the naphthol and naphtholate (Fig. 5 and Fig. S13 in the ESI†), the use of the Förster cycle[53] and the value of pK_a = 9.5,[46] the pK_a^* can be approximated as $pK_a^* \approx 0$ (the reported value for

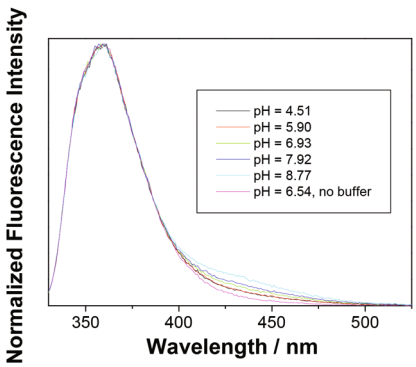

Fig. 5 Normalized fluorescence spectra (λ_{ex} = 310 nm) of **4a** in $CH_3CN–H_2O$ (1 : 1) at different pH values (0.05 M sodium phosphate buffer was used).

2-naphthol pK_a* = 2.8).[46] Note that the Förster analysis gives inaccurate values of the pK_a*. Nevertheless, the difference of the emission maxima for the naphthol and naphtholate indicate a significant increase of the acidity of bis-naphthols in S_1. Non-observation of the naphtholate emission is an indication that ESPT takes place very inefficiently. That is, ESPT is in competition with the other nonradiative pathway from S_1, presumably SB-CS.

Single photon counting measurements were conducted for bis-naphthol derivatives **4a** and **4e** to measure singlet excited state lifetimes, and to verify if ESPT in the aqueous solvent takes place. The samples were excited at 267 nm and the decay was measured in CH_3CN or in CH_3CN–H_2O (1 : 1) in the presence of sodium phosphate buffer (0.05 M, pH = 7.0) where a difference was anticipated due to ESPT taking place in the aqueous solvent. The fluorescence decay in CH_3CN for both **4a** and **4e** was fit to a single exponential function revealing the S_1 lifetime (Table 3 and Fig. S14 in the ESI†). The similar S_1 lifetimes, which do not depend on the alkyl chain length, are in accord with the similar values of quantum yields of fluorescence for all derivatives **4**. On the other hand, in buffered aqueous solution the decay was fit to a sum of two exponentials where the contribution of the decay time depended on the detection wavelength (see Fig. S15 in the ESI†). Most importantly, at wavelengths >460 nm where the naphtholate emits, the pre-exponential factor attributed to the shorter decay time was negative, indicating the formation of the species in S_1. Therefore, this shorter decay time was assigned to the emission of naphthol, whereas the longer decay component was assigned to the emission of naphtholate (Table 3).

Laser flash photolysis

LFP experiments were conducted to detect QMs and other plausible intermediates formed upon excitation of **4** (for all LFP data see Fig. S16–S38 in the ESI†). Similar to the fluorescence measurements, the transient spectra were collected in CH_3CN or in buffered CH_3CN–H_2O (1 : 1) where the differences were anticipated due to proton transfer to the solvent. Moreover, prior to the measurements, the solutions were purged with Ar or O_2, and it was anticipated that O_2 would quench the plausible triplet excited state, radicals and radical anions, but not radical cations and QMs.

In the N_2-purged CH_3CN solution of **4a** we detected two short-lived transients absorbing practically over the whole visible spectral region (Fig. S17 in the ESI†), with a maximum at ≈450 nm: τ_{Ar} = 320 ± 20 ns and at ≈350 and 550 nm: τ_{Ar} = 54 ± 1 ns (Fig. S19 in the ESI†). In addition, more persistent transient absorption was detected at ≈350 nm which was fit to a sum of two exponents with the decay times of τ_{Ar} = 26 ± 2 μs and 280 ± 10 μs (Fig. S20 in the ESI†). Purging the solution with O_2 did not change the spectra (Fig. 6), but it changed the decay kinetics. Thus, the transient with a maximum at 450 nm was quenched by O_2 (τ_{O_2} = 130 ± 10 ns), whereas the transient absorbing at 550 nm had a similar lifetime to the one detected in Ar-purged solution (τ_{O_2} = 48 ± 1 ns). The decay kinetics for the long-lived transient absorbing at 350 nm was fit to a sum of two exponents with decay times of τ_{O_2} = 60 ± 2 μs and 720 ± 70 μs. Based on the anticipated SB-CS and observed quenching by O_2, we tentatively assigned the short-lived transient at 450 nm to the naphthol radical anion, whereas the transient absorbing at 350 and 550 nm was tentatively assigned to the naphthol radical cation. The assignment is based on the quenching by O_2 and the comparison with the published spectra for naphthalene radical cations[54] and radical anions,[55] which generally overlap.[56,57] The transient absorbing at 350 nm whose absorption stretches to a longer wavelength with the lifetime in tens of microseconds was assigned to the naphthoxyl radical (τ_{O_2} = 60 ± 2 μs), based on a comparison with the precedent spectra in the literature[58] and the fact that phenol radical cations deprotonate giving phenoxyl radicals.[59] The longest lived transient with a lifetime of 720 μs was assigned to quinone methide, based on a comparison with the precedent spectra.[42] However, the lifetime of 720 μs is only a lower limit, and the precise lifetime could not be determined with the set-up used.

In the Ar- and O_2-purged aqueous buffered solution of **4a** we detected similar spectra to those in CH_3CN solution with the short-lived transient absorbing over the whole visible part of the spectrum (Fig. S22 and S23 in the ESI†). At ≈350 nm and λ > 550 nm a very short-lived transient was detected with a lifetime at the limits of detection (5–10 ns) that were assigned to the radical cation. Fast decay in aqueous solution is in

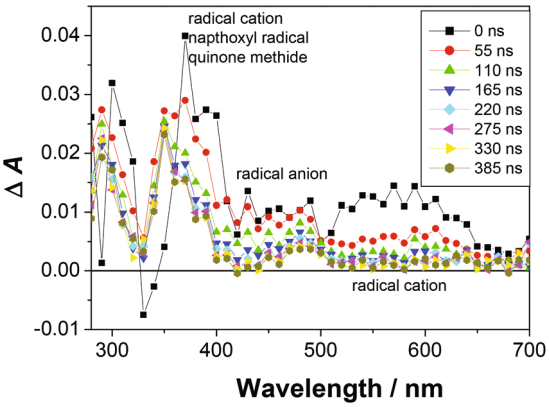

Fig. 6 Transient absorption spectra of **4a** (c = 5.05 × 10^{-5} M) in O_2-purged CH_3CN.

Table 3 Decay times measured by SPC

Compound	τ (CH_3CN)/ns	τ (CH_3CN–H_2O)[a]/ns
4a	7.0 ± 0.3	4.9 ± 0.4 2.1 ± 0.2[b]
4e	6.7 ± 0.3	4.5 ± 0.4 3.0 ± 0.3[b]

[a] Measurements were performed in CH_3CN–H_2O (1 : 1) in the presence of sodium phosphate buffer (0.05 M, pH = 7.0). [b] Decay time corresponding to naphthol with a negative pre-exponential factor for decay measured at >460 nm where the naphtholate formed in S_1 emits.

accord with the deprotonation to the phenoxyl radical in that solvent. In addition, we detected a transient absorbing at 400–500 nm that was quenched by O_2 and assigned to the radical anion with the lifetimes $\tau_{Ar} = 120 \pm 10$ ns and $\tau_{O_2} = 83 \pm 3$ ns (Fig. S24 in the ESI†). At longer delays after the laser pulse, at 350 nm we detected the QM that decayed with unimolecular kinetics and approximate lifetime values of $\tau_{Ar} = 2.1 \pm 0.6$ ms and $\tau_{O_2} = 2.8 \pm 0.8$ ms (Fig. S25 in the ESI†). The assignment is additionally corroborated by a quenching with NaN_3 (c = 0.010 M) when the decay was faster (τ = 230 ± 80 μs). A proper quenching plot could not be obtained due to the very low intensity of the signal at a long time-scale, at the limits of detection of the set-up used. However, from two decay times, an approximate value of the quenching constant with an azide is $k_q \approx 4 \times 10^5$ M^{-1} s^{-1}, which is about 10 times that reported by Popik,[42] and about ten times lower than that reported by us for sterically congested naphthalene QMs.[37]

The transient absorption spectra of **4e** are similar to those measured for **4a** at the long time-scale, but at the short time-scale we observed some differences (Fig. S28 and S29 in the ESI†). In Ar and O_2-purged CH_3CN solution we detected only one short-lived transient absorbing over the whole spectrum with the maximum at ≈350 nm and the lifetime of $\tau \approx 10$ ns. It probably corresponds to radical ions, but we cannot unambiguously say if it corresponds to the radical cation, the radical anion, or both species. On the other hand, in aqueous buffered solution, under Ar, the transient absorbance was fit to a single exponential function (*e.g.* 470 nm $\tau_{Ar} \approx 23 \pm 1$ ns), whereas in O_2-purged solution, depending on the detection wavelength the decay of the transient absorbance was fit to a single exponential (at 450 nm, $\tau_{O_2} \approx 24 \pm 1$ ns) or two-exponential function ($\tau_{550} \approx 6 \pm 1$ ns and 43 ± 1 ns). The short-lived transient, which can be detected at higher wavelengths (>550 nm, τ < 10 ns), probably corresponds to the radical cation, whereas the longer-lived transient probably corresponds to the radical anion ($\tau \approx 20$–40 ns). That is, deprotonation of the radical cation in aqueous solvent should be fast and give naphthoxyl radicals.[58] On the other hand, we anticipate that radical anions should not be very basic and prone to protonation since the protonation would form unstable carbon-centered radicals with the loss of aromaticity from the naphthalene. After the decay of short-lived transients, at a long delay after the laser pulse we detected the QM with the maximum of absorption at 350 nm. It decayed with unimolecular kinetics and the lifetime of $\tau_{O_2} \approx$ 1–2 ms. Due to the very low intensity of the transient assigned to the QM we could not perform the quenching experiment. Consequently, LFP experiments allowed for the detection of radical ions formed in the SB-CS process, as well as the QM formed from the photodehydration.

Photochemical reaction mechanism

Based on the preparative irradiation experiments, and UV-vis, fluorescence and LFP study, we can propose plausible reaction pathways for the bis-naphthol derivatives, which are also probably similar for bis-anthrols. Light absorption excites one naphthol chromophore moiety, which undergoes three competitive photochemical pathways. The SB-CS[43] and photodehydration[34] probably take place in an ultrafast manner delivering radical ions **4-RIP** and **4-QM**, respectively (Scheme 4). On the other hand, the ESPT to the solvent giving the naphtholate is much slower (plausible rate constant for deprotonation $k = 7 \times 10^7$ s^{-1}),[46] and, therefore, takes place inefficiently. Thus, naphtholate emission ($4O^-$) can be detected only at pH > 7, even though pK_a^* is probably close to 0, as estimated from the Förster cycle. After the population of **4-RIP**, the plausible pathways are back electron transfer (beT), which recovers the starting bis-naphthols **4** and probably represents the major pathway due to which all other processes take place inefficiently. The other plausible pathway for **4-RIP** is deprotonation giving naphthoxyl radicals, which were detected by LFP. Even though radical anions are generally basic, their protonation in

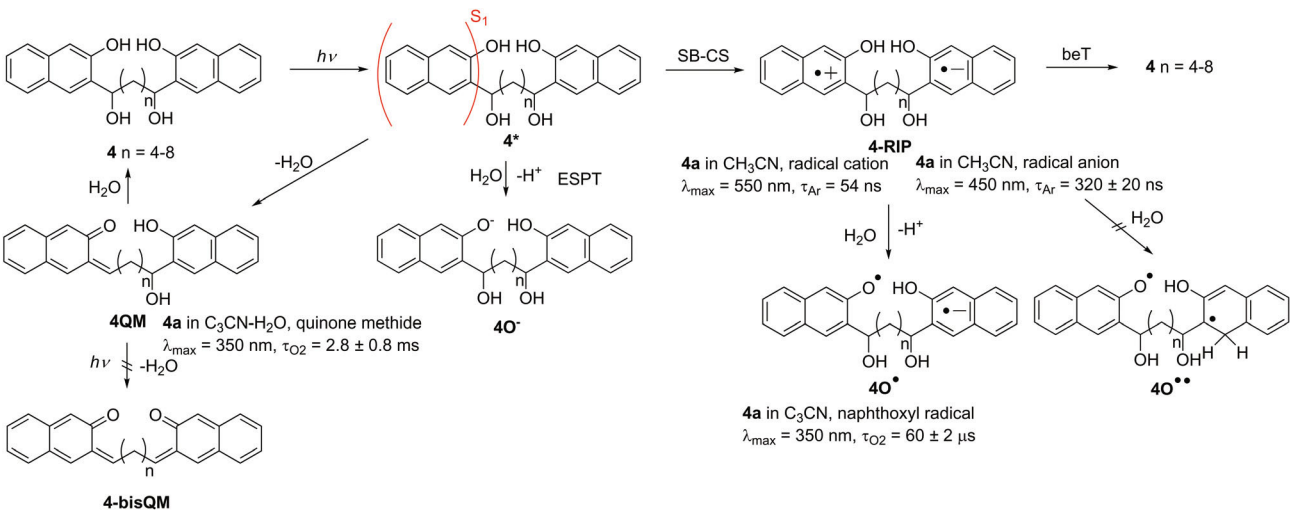

Scheme 4 Plausible photochemical reaction pathways for bis-naphthols.

this case is less probable since it would deliver the less stable C-centered radical.

We imply that photodehydration in **4** probably takes place in an ultrafast manner, since it has to compete with SB-CS. Ultrafast dehydration has been described for phenol derivatives.[34] The dehydration delivers **4-QM**, which was detected by LFP. However, formation of **4-bisQM** is not a probable pathway since it would require absorption of light by an intermediate **4QM** and a secondary dehydration reaction. More probable is a hydration of **4QM**, a ubiquitous decay pathway of QMs,[60] recovering **4**.

In conclusion, we have demonstrated that bis-naphthols **4** undergo dehydration and deliver QMs. The analogous mechanistic scheme can tentatively be proposed for bis-anthrols **5**, although the only evidence we have is photomethanolysis. Furthermore, it should be noted that bis-anthrols **5** undergo additional photochemical pathways since they form many photochemical products and these pathways are not disclosed here.

Non-covalent binding to bovine and human serum albumin (BSA and HSA)

Serum albumins are proteins that are known to bind different hydrophobic guest molecules.[61] Furthermore, it has recently been demonstrated that human serum albumin (HSA) binds naphthalene QM precursors, which then leads to the alkylation at Lys residues.[62] To probe for the noncovalent binding of bis-naphthols **4** to BSA and HSA we performed fluorescence titrations for **4a** with both proteins in (1 : 1) CH_3CN–aqueous sodium phosphate buffer, c = 0.05 M, pH = 7.0. Upon addition of protein to the solution of bis-naphthol **4a**, the fluorescence was quenched (for BSA see Fig. 7, and for HSA see Fig. S39–S43 in the ESI†). Multivariate nonlinear regression analysis by using the Specfit program and the model based on the 1 : 2 (protein : **4a**) stoichiometry provided the best fit with the complex stability constant $\log K_{12}$ values of 8.10 ± 0.04 for BSA and 8.13 ± 0.03 for HSA. At a higher protein concentration, in the fluorescence spectra of **4a** the bend at ≈450 nm becomes more visible indicating that **4a** undergoes more efficient ESPT in the protein complex. The finding can be rationalized by the well-known binding of naphthols in the hydrophobic pockets of the protein,[63] which contain H_2O molecules to enable ESPT, but a less polar environment reduces the quantum yield of SB-CS.

To initiate the photodehydration of bis-naphthols in the presence of proteins, the irradiation was performed in a reactor equipped with lamps with the maximum of emission at 350 nm. These lamps provide excitation in the range 320–400 nm and allow for the selective excitation of bis-naphthols **4**, with the minimal absorption of light by the protein. Irradiation of the solutions containing the protein complexes resulted in further fluorescence quenching, suggesting that molecule **4a** reacts photochemically with the proteins (see Fig. S40 and S43 in the ESI†). Analysis of the solution after the irradiation by MALDI-TOF/TOF mass spectrometry indicated that the photochemical alkylation of the proteins took place. The observed molecular weight of BSA and HSA was increased by 325 and 390, respectively. The MS analyses indicated covalent biding of one molecule **4a** (molecular weight: 402) to the proteins, with the observed increases in the molecular weight within the acceptable error of the method.[64]

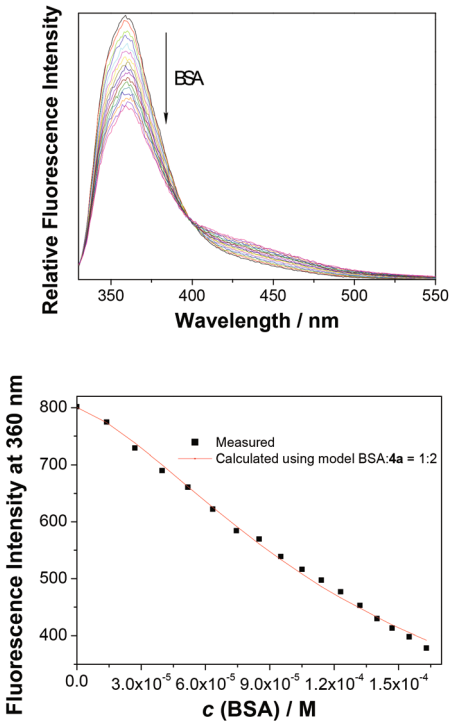

Fig. 7 Fluorescence spectra (λ_{ex} = 320 nm) of **4a** (c = 1.49 × 10^{-5} M) in aqueous sodium phosphate buffer (c = 0.05 M, pH 0 7.0) : CH_3CN 1 : 1, in the presence of an increasing concentration of BSA (c = 0–1.63 × 10^{-4} M) (top); and dependence of the fluorescence intensity at 360 nm on the BSA concentration (bottom); the dots correspond to the experimental values, whereas the red line is the calculated fluorescence intensity by using the Specfit program and complex stoichiometry model 1 : 2 (protein : **4a**).

Photocytotoxicity study

The antiproliferative effect of the photogenerated QMs on three cancer cell lines H1299 (lung carcinoma), MCF-7 (breast adenocarcinoma) and SUM159 (pleomorphic breast carcinoma), was investigated with bis-naphthols and bis-anthrols. A psoralen derivative was used as a positive reference compound which is known to exhibit antiproliferative activity after photoactivation.[18] Cells were incubated with the compounds and kept in a cell incubator in the dark for 3 days, or irradiated each day (at 350 nm for 5 min for naphthols or at 420 nm for 10 min for anthrols). The activities expressed as GI_{50} (concentration that causes 50% inhibition of the cell growth) are compiled in Table 4. Without the irradiation, all compounds exert mild antiproliferative activity in a micromolar concentration range, without a specific effect with respect to the cell type. Irradiation induced up to a 10-fold enhancement of the activity. Bis-naphthol derivative **4a** with the shortest spacer length between the chromophores exerts the highest cyto-

Table 4 GI_{50} values (in μM)[a] induced with compounds **4**, **5** and psoralen derivative with and without irradiation

Comp.	H1299	H1299 irr	SUM159	SUM159 irr	MCF-7	MCF-7 irr
4a	**14.7 ± 0.7**	**3 ± 2**	**13.9 ± 0.5**	**1.79 ± 0.01**	**13 ± 1**	**2.0 ± 0.5**
4b	15.2 ± 0.3	9 ± 4	14.84 ± 0.02	5 ± 1	14.5 ± 0.7	11 ± 1
4c	16.0 ± 0.3	8 ± 5	15.74 ± 0.05	4.1 ± 0.4	15 ± 1	7 ± 4
4d	11.72 ± 0.03	5 ± 1	7 ± 2	3.6 ± 0.3	1.4 ± 0.4	3.2 ± 0.5
4e	15 ± 3	13 ± 1	10 ± 4	4.4 ± 0.3	13 ± 3	4 ± 1
5a	**23 ± 12**	**0.7 ± 0.2**	**15 ± 5**	**0.2 ± 0.04**	**16± 5**	**1 ± 1**
5e	40 ± 20	3 ± 1	9 ± 2	1.6 ± 0.4	3 ± 2	1 ± 1
Psoralen	>100	<0.01	>100	<0.01	3 ± 2	<0.01

[a] Concentration that causes 50% inhibition of tumor cell growth (entries commented on in the text are marked in bold).

toxicity upon irradiation toward all three cell lines tested. Similarly, bis-anthrol derivative **5a** experiences the most pronounced enhancement of the antiproliferative activity upon irradiation of cells, particularly on H1299 and SUM159.

Conclusions

Upon photoexcitation, bis-naphthols **4** undergo competitive processes, with the SB-CS giving rise to radical ions and photodehydration delivering QMs. The intermediates in these processes were detected by LFP. The ESPT takes place, but it is inefficient since it takes place slower. The antiproliferative activity of bis-naphthols **4** and bis-anthrols **5** upon irradiation was investigated on human cancer cell lines, which were kept in the dark or irradiated. An enhancement of the antiproliferative activity upon irradiation was observed and may be connected to the photochemical formation of QMs. However, these QMs do not induce DNA cross-linking. A more plausible mechanism of the enhancement of antiproliferative activity is alkylation of proteins in the cell cytoplasm. The mechanistic investigation presented herein is particularly important since it unravels the plausible pathways for bis-chromophoric systems that could be used in the development of agents for phototreatment of cancer.

Experimental

General

Chemicals for the synthesis were purchased from the usual suppliers. Solvents for the synthesis and chromatographic separations were used as received (p.a. grade). The solvent (ether) for Grignard reactions was dried over sodium and freshly distilled. ^{1}H and ^{13}C NMR spectra were recorded on Bruker Avance III 600, Bruker Avance DRX 500, Bruker Avance DPX 300 (equipped with a 5 mm BBI probe) and Bruker Avance AV400 (equipped with a 5 mm BBO probe) spectrometers using standard Bruker pulse sequences. All samples were recorded at 25 °C using DMSO-d_6 and $CDCl_3$ as solvents and TMS as the internal standard. For the sample analysis a Waters Acquity UPLC coupled with an SQD mass spectrometer with an Acquity UPLC BEH C18 (50 × 2.1 mm, 1.7 μm packing) column was used. Mobile phase was A: 10 mM aqueous solution of ammonium bicarbonate (adjusted to pH 10 with ammonia), mobile phase B: acetonitrile. The gradient was 0.0 min, 97% A, 3% B; 1.5 min, 100% B; 1.9 min, 100% B; 2.0 min, 97% A, 3% B, the flow rate was 0.9 mL min^{-1} and the column temperature was 40 °C. UV detection was performed from 210 nm to 350 nm. MS conditions: Ionization mode was alternate-scan positive and negative electrospray (ES^+/ES^-); scan range: 100 to 1000 AMU. Alternatively, a Shimadzu HPLC system equipped with a diode-array detector and a Phenomenex Luna 3u C18(2) column was used. The mobile phase was 75% CH_3OH and 15% H_2O and the flow rate was 1.0 mL min^{-1}. The chromatographic separations were performed on a flash chromatography apparatus using commercially available Interchim, prepacked silica cartridges. Analytical thin layer chromatography was performed on Silica Gel 60 F254 aluminium sheets (Merck). For preparative HPLC purification a Waters Mass Directed Autopurification System consisting of a Waters 2767 Sample Manager, a Waters Column Fluidic Organizer, a Waters 515 HPLC Pump, a Waters 2525 Binary Gradient Module, a Waters Pump Control Module II, a Waters 2996 PDA Detector and a Waters Micromass ZQ was used. The column for separation processes was XBridge Prep. C18 (150 × 30 mm, 5 μm packing). The mobile phases for the separation processes were A: 10 mM aqueous solution of ammonium bicarbonate (adjusted to pH 10 with ammonia) and mobile phase B: acetonitrile. The gradient for the separation processes was 0.0 min, 70% A, 30% B; 10 min, 35% A, 65% B; 10 min, 0% A, 100% B; 15 min, 0% A, 100% B; flow rate: 50 mL min^{-1}. MS conditions: Ionization mode – positive and negative electrospray (ES^+/ES^-); scan range: 105 to 1000 AMU. Melting points were determined using a Mikroheiztisch apparatus and were not corrected. HRMS was performed on an Applied Biosystems Voyager DE STR MALDI-TOF/TOF instrument. In the irradiation experiments, CH_3OH and CH_3CN were of HPLC grade, and ultrapure water (Milli-Q H_2O, Millipore) was used. ct-DNA was purchased from Aldrich. The preparation of precursor molecules, carbaldehydes **6** and **8** is fully described in the ESI.†

Preparation of bis-naphthol 7 and bis-anthrol 9 derivatives – general procedure

In a two neck flask (50 mL), equipped with a condenser and a septum, under an inert N_2 atmosphere, Mg (4.5 mmol), dry diethyl ether (4.5 mL) and a crystal of iodine were added. A

small quantity of the solution of 1,*n*-dibromoalkane (2.25 mmol) in ether (11 mL) was added dropwise through the septum *via* a syringe. When the reaction was initiated by heating, the remaining dibromoalkane solution was added at rt or with moderate heating. After the addition was complete, the reaction mixture was heated at the reflux temperature for 1 h, cooled to rt, and a solution of the protected carbaldehyde (**6** or **8**, 1 mmol) in dry ether (5 mL) was added dropwise. After 2 h of stirring at rt, the reaction mixture was quenched with saturated aqueous NH_4Cl solution (15 mL). The mixture was transferred to a separation funnel, the layers were separated and the aqueous layer was extracted with ethyl acetate (3 × 15 mL). The organic extracts were dried over anhydrous $MgSO_4$ and filtered, and the solvent was removed on a rotary evaporator. The residue was subjected to chromatography on a column of silica gel using the gradient method from 0 to 13% of ethyl acetate/cyclohexane as the eluent.

1,6-Bis[3-(*tert*-butyldimethylsilyloxy)-2-naphthyl]hexane-1,6-diole (7a)

According to the general procedure, the Grignard reagent was prepared from 1,4-dibromobutane (0.37 mL, 3.06 mmol) and Mg (0.15 g, 6.13 mmol) in dry ether. In the reaction with the protected aldehyde (**6**, 390 mg, 1.36 mmol) the product (217 mg, 51%) was obtained in the form of a colorless solid.

Mp 44–45 °C; ^{1}H NMR ($CDCl_3$, 400 MHz) δ/ppm: 7.80 (s, 2H), 7.74 (d, 2H, J = 7.9 Hz), 7.64 (dd, 2H, J = 8.2 Hz, J = 0.4 Hz), 7.39 (dt, 2H, J = 8.3 Hz, J = 1.3 Hz), 7.31 (dt, 2H, J = 8.2 Hz, J = 1.2 Hz), 7.11 (s, 2H), 5.05 (br. s, 2H), 2.30 (br. s, 2H), 1.95–1.72 (m, 4H), 1.67–1.58 (m, 2H), 1.52–1.43 (m, 2H), 1.03 (s, 18H), 0.33 (s, 6H), 0.32 (s, 6H); ^{13}C NMR ($CDCl_3$, 100 MHz) δ/ppm: 151.2, 136.4, 133.5, 128.9, 127.7, 126.2, 125.9, 125.8, 123.9, 113.1, 70.4, 70.3 37.5, 26.9, 26.2, 26.2, 25.9, 18.3, −3.9, −4.1.

1,7-Bis[3-(*tert*-butyldimethylsilyloxy)-2-naphthyl]heptane-1,7-diole (7b)

According to the general procedure, the Grignard reagent was prepared from 1,5-dibromopentane (1.07 mL, 7.86 mmol) and Mg (382 mg, 15.71 mmol) in dry ether. In the reaction with the protected aldehyde (**6**, 300 mg, 1.05 mmol) the product (736 mg, 65%) was obtained in the form of a colorless solid.

Mp 57–58 °C; ^{1}H NMR ($CDCl_3$, 400 MHz) δ/ppm: 7.80 (s, 2H), 7.74 (d, 2H, J = 8.0 Hz), 7.64 (d, 2H, J = 8.3 Hz), 7.39 (dt, 2H, J = 8.0 Hz, J = 1.2 Hz), 7.31 (dt, 2H, J = 8.0 Hz, J = 1.1 Hz), 7.11 (s, 2H), 5.10–4.99 (m, 2H), 2.30 (d, 2H, J = 4.7 Hz), 1.92–1.68 (m, 4H), 1.57–1.49 (m, 2H), 1.42–1.31 (m, 2H), 1.04 (s, 18H), 0.34 (s, 6H), 0.33 (s, 6H); ^{13}C NMR ($CDCl_3$, 100 MHz) δ/ppm: 151.2, 136.5, 133.5, 128.9, 127.7, 126.2, 125.9, 125.7, 123.9, 113.1, 70.4, 37.6, 29.8, 26.9, 26.2, 25.8, 18.3, −3.9, −4.1.

1,8-Bis[3-(*tert*-butyldimethylsilyloxy)-2-naphthyl]octane-1,8-diole (7c)

According to the general procedure, the Grignard reagent was prepared from 1,6-dibromohexane (0.36 mL, 2.36 mmol) and Mg (115 mg, 4.71 mmol) in dry ether. In the reaction with the protected aldehyde (**6**, 1.00 g, 3.49 mmol) the product (267 mg, 78%) was obtained in the form of a colorless solid.

Mp 41–42 °C; ^{1}H NMR ($CDCl_3$, 400 MHz) δ/ppm: 7.80 (s, 2H), 7.75 (dd, 2H, J = 7.9 Hz, J = 0.5 Hz), 7.65 (d, 2H, J = 8.2 Hz), 7.39 (dt, 2H, J = 8.0 Hz, J = 1.4 Hz), 7.31 (dt, 2H, J = 8.0 Hz, J = 1.4 Hz), 7.11 (s, 2H), 5.09–5.00 (m, 2H), 2.29 (d, 2H, J = 4.7 Hz), 1.92–1.69 (m, 4H), 1.57–1.48 (m, 2H), 1.41–1.26 (m, 6H), 1.03 (s, 18H), 0.34 (s, 6H), 0.33 (s, 6H); ^{13}C NMR ($CDCl_3$, 100 MHz) δ/ppm: 151.2, 136.5, 133.5, 128.9, 127.7, 126.2, 125.9, 125.7, 123.9, 113.1, 70.4, 37.6, 29.7, 29.7, 26.9, 26.1, 25.9, 18.3, −3.9, −4.1.

1,9-Bis[3-(*tert*-butyldimethylsilyloxy)-2-naphthyl]nonane-1,9-diole (7d)

According to the general procedure, the Grignard reagent was prepared from 1,7-dibromoheptane (0.67 mL, 3.93 mmol) and Mg (191 mg, 7.86 mmol) in dry ether. In the reaction with the protected aldehyde (**6**, 500 mg, 1.75 mmol) the product (370 mg, 63%) was obtained in the form of a colorless solid.

Mp 42–43 °C; ^{1}H NMR ($CDCl_3$, 400 MHz) δ/ppm: 7.81 (s, 2H), 7.75 (dd, 2H, J = 8.0 Hz, J = 0.5 Hz), 7.64 (dd, 2H, J = 8.2 Hz, J = 0.4 Hz), 7.42–7.35 (m, 2H), 7.35–7.29 (m, 2H), 7.11 (s, 2H), 5.09–5.00 (m, 2H), 2.28 (d, 2H, J = 4.7 Hz), 1.92–1.68 (m, 4H), 1.55–1.46 (m, 2H), 1.42–1.19 (m, 8H), 1.04 (s, 18H), 0.34 (s, 6H), 0.33 (s, 6H); ^{13}C NMR ($CDCl_3$, 100 MHz) δ/ppm: 151.3, 136.6, 133.5, 128.9, 127.7, 126.2, 125.9, 125.7, 126.9, 113.1, 70.4, 37.7, 29.7, 29.6, 26.1, 25.9, 18.3, −4.0, −4.1.

1,10-Bis[3-(*tert*-butyldimethylsilyloxy)-2-naphthyl]decane-1,10-diole (7e)

According to the general procedure, the Grignard reagent was prepared from 1,8-dibromooctane (0.56 mL, 3.06 mmol) and Mg (149 mg, 6.13 mmol) in dry ether. In the reaction with the protected aldehyde (**6**, 390 mg, 1.36 mmol) the product (227 mg, 49%) was obtained in the form of a colorless solid.

Mp 40–41 °C; ^{1}H NMR ($CDCl_3$, 400 MHz) δ/ppm: 7.81 (s, 2H), 7.75 (dd, 2H, J = 8.0 Hz, J = 0.5 Hz), 7.64 (dd, 2H, J = 8.2 Hz, J = 0.4 Hz), 7.42–7.35 (m, 2H), 7.35–7.29 (m, 2H), 7.11 (s, 2H), 5.09–5.00 (m, 2H), 2.28 (d, 2H, J = 4.8 Hz), 1.92–1.68 (m, 4H), 1.55–1.46 (m, 2H), 1.42–1.23 (m, 10H), 1.05 (s, 18H), 0.35 (s, 6H), 0.33 (s, 6H); ^{13}C NMR ($CDCl_3$, 100 MHz) δ/ppm: 151.3, 136.6, 133.5, 128.9, 127.7, 126.2, 125.9, 125.7, 123.9, 113.1, 70.4, 37.7, 29.7, 29.6, 26.1, 25.9, 18.3, −3.9, −4.1.

1,6-Bis[3-(*tert*-butyldimethylsilyloxy)-2-anthryl]hexane-1,6-diole (9a)

According to the general procedure, the Grignard reagent was prepared from 1,4-dibromobutane (0.24 mL, 2.01 mmol) and Mg (98 mg, 4.01 mmol) in dry ether. In the reaction with the protected carbaldehyde (**8**, 300 mg, 0.89 mmol) the product (129 mg, 40%) was obtained in the form of a beige solid.

Mp 77–78 °C; ^{1}H NMR ($CDCl_3$, 500 MHz) δ/ppm: 8.35 (s, 2H), 8.23 (s, 2H), 8.04–7.83 (m, 6H), 7.50–7.37 (m, 4H), 7.29 (s, 2H), 5.16–5.06 (m, 2H), 2.06–1.80 (m, 5H), 1.78–1.50 (m, 5H), 1.07 (s, 18H), 0.41 (s, 6H), 0.40 (s, 6H); ^{13}C NMR ($CDCl_3$, 125 MHz) δ/ppm: 151.1, 137.3, 131.9, 131.8, 130.6, 128.2,

128.1, 127.5, 126.1, 125.8, 125.3, 124.4, 123.6, 111.5, 70.6, 37.4, 26.25, 26.21, 25.8, 18.3, −3.9, −4.1.

1,10-Bis[3-(*tert*-butyldimethylsilyloxy)-2-anthryl]decan-1,6-diole (9e)

According to the general procedure, the Grignard reagent was prepared from 1,8-dibromooctane (0.37 mL, 2.01 mmol) and Mg (98 mg, 4.01 mmol) in dry ether. In the reaction with the protected carbaldehyde (**8**, 300 mg, 0.89 mmol) the product (152 mg, 43%) was obtained in the form of a beige solid.

Mp 70–71 °C; ^{1}H NMR ($CDCl_3$, 500 MHz) δ/ppm: 8.33 (s, 2H), 8.23 (s, 2H), 7.97 (s, 2H), 7.93 (dd, 4H, J = 13.0 Hz, J = 8.2 Hz), 7.45–7.34 (m, 4H), 7.23 (s, 2H), 5.11–5.02 (m, 2H), 2.13 (br. s, 2H), 1.96–1.86 (m, 2H), 1.85–1.75 (m, 2H), 1.64–1.49 (m, 4H), 1.38–1.24 (m, 8H), 1.06 (s, 18H), 0.40 (s, 6H), 0.38 (s, 6H); ^{13}C NMR ($CDCl_3$, 125 MHz) δ/ppm: 151.2, 137.5, 131.9, 131.8, 130.6, 128.2, 128.1, 127.5, 126.1, 125.7, 125.3, 124.4, 123.6, 11.4, 70.7, 37.5, 29.7, 26.9, 26.1, 25.8, 18.3, −3.9, −4.1.

Removal of the TBDMS protective group – general procedure

A flask (25 mL) equipped with a septum was charged with TBDMS-protected bis-naphthol **7** or bis-anthrol **9** (1 mmol) and THF (10 mL) under an inert N_2 atmosphere. The mixture was cooled to 0 °C, and a solution of TBAF in THF (2.2 mmol, 1 M) was added dropwise. The stirring was continued at 0 °C for 20 min, and then at rt for 30 min. To the reaction mixture, water (15 mL) was added and extraction with ethyl acetate (3 × 15 mL) was carried out. The combined extracts were dried over anhydrous $MgSO_4$ and filtered, and the solvent was removed using a rotary evaporator. The crude residue was subjected to chromatography on a silica gel column using the gradient method from 0 to 10% of ethyl acetate/cyclohexane as the eluent. In the case of bis-anthrol compounds, purification was performed by trituration of the crude product with several portions of cold ethyl acetate and ether.

1,6-Bis(3-hydroxy-2-naphthyl)hexane-1,6-diol (4a)

According to the general procedure from **7a** (217 mg, 0.34 mmol) the reaction furnished the product (92 mg, 66%) in the form of a colorless solid.

Mp 178–180 °C; ^{1}H NMR (DMSO-d_6, 500 MHz) δ/ppm: 9.75 (br. s, 2H), 7.80 (s, 2H), 7.73 (d, 2H, J = 7.5 Hz), 7.63 (d, 2H, J = 7.5 Hz), 7.35–7.28 (m, 2H), 7.25–7.19 (m, 2H), 7.08 (s, 2H), 5.12 (br. s, 2H), 4.97–4.88 (m, 2H), 1.79–1.66 (m, 2H), 1.59–1.29 (m, 6H); ^{13}C NMR (DMSO-d_6, 125 MHz) δ/ppm: 152.9, 135.8, 135.7, 133.2, 127.7, 127.4, 125.4, 125.3, 124.9, 122.6, 108.3, 67.29, 67.26, 37.9, 25.6; HRMS (MALDI TOF/TOF) calcd for $C_{26}H_{26}O_4$ $[M + Na]^+$ 425.1723 found 425.1729.

1,7-Bis(3-hydroxy-2-naphthyl)heptane-1,7-diol (4b)

According to the general procedure from **7b** (730 mg, 1.13 mmol) the reaction furnished the product (425 mg, 90%) in the form of a colorless solid.

Mp 168–170 °C; ^{1}H NMR (DMSO-d_6, 400 MHz) δ/ppm: 9.73 (s, 2H), 7.80 (s, 2H), 7.74 (d, 2H, J = 8.3 Hz), 7.62 (d, 2H, J = 7.9 Hz), 7.35–7.28 (m, 2H), 7.25–7.19 (m, 2H), 7.08 (s, 2H), 5.10 (d, 2H, J = 4.3 Hz), 4.98–4.89 (m, 2H), 1.79–1.64 (m, 2H), 1.58–1.45 (m, 2H), 1.45–1.17 (m, 6H); ^{13}C NMR (DMSO-d_6, 100 MHz) δ/ppm: 152.8, 135.8, 133.2, 127.7, 127.4, 125.4, 125.3, 124.9, 122.6, 108.3, 67.2, 37.9, 29.2, 25.6; HRMS (MALDI TOF/TOF) calcd for $C_{27}H_{28}O_4$ $[M + Na]^+$ 439.1880 found 439.1860.

1,8-Bis(3-hydroxy-2-naphthyl)octane-1,8-diol (4c)

According to the general procedure from **7c** (267 mg, 0.41 mmol) the reaction furnished the product (170 mg, 97%) in the form of a colorless solid.

Mp 162–163 °C; ^{1}H NMR (DMSO-d_6, 400 MHz) δ/ppm: 9.74 (br. s, 2H), 7.80 (s, 2H), 7.74 (d, 2H, J = 8.2 Hz), 7.62 (d, 2H, J = 7.9 Hz), 7.36–7.28 (m, 2H), 7.26–7.18 (m, 2H), 7.08 (s, 2H), 5.11 (br. s, 2H), 4.98–4.89 (m, 2H), 1.77–1.64 (m, 2H), 1.58–1.45 (m, 2H), 1.45–1.12 (m, 8H); ^{13}C NMR (DMSO-d_6, 100 MHz) δ/ppm: 152.8, 135.8, 133.2, 127.7, 127.4, 125.4, 125.3, 124.9, 122.5, 108.3, 67.2, 37.9, 29.2, 25.5; HRMS (MALDI TOF/TOF) calcd for $C_{28}H_{30}O_4$ $[M + Na]^+$ 453.2036 found 453.2039.

1,9-Bis(3-hydroxy-2-naphthyl)nonane-1,9-diol (4d)

According to the general procedure from **7d** (370 mg, 0.55 mmol) the reaction furnished the product (200 mg, 82%) in the form of a colorless solid.

Mp 112–113 °C; ^{1}H NMR (DMSO-d_6, 400 MHz) δ/ppm: 9.73 (s, 2H), 7.81 (s, 2H), 7.73 (d, 2H, J = 7.9 Hz), 7.62 (d, 2H, J = 8.0 Hz), 7.36–7.28 (m, 2H), 7.26–7.19 (m, 2H), 7.08 (s, 2H), 5.11 (br. s, 2H), 4.98–4.86 (m, 2H), 1.79–1.64 (m, 2H), 1.58–1.44 (m, 2H), 1.45–1.15 (m, 10H); ^{13}C NMR (DMSO-d_6, 100 MHz) δ/ppm: 152.8, 135.8, 133.2, 127.7, 127.4, 125.4, 125.3, 124.9, 122.6, 108.3, 67.2, 37.8, 29.2, 29.1, 25.4; HRMS (MALDI TOF/TOF) calcd for $C_{29}H_{32}O_4$ $[M + Na]^+$ 467.2192 found 467.2190.

1,10-Bis(3-hydroxy-2-naphthyl)decane-1,10-diol (4e)

According to the general procedure from **7e** (226 mg, 0.33 mmol) the reaction furnished the product (129 mg, 85%) in the form of a colorless solid.

Mp 152–155 °C; ^{1}H NMR (DMSO-d_6, 400 MHz) δ/ppm: 9.73 (s, 2H), 7.81 (s, 2H), 7.73 (d, 2H, J = 7.9 Hz), 7.61 (d, 2H, J = 7.8 Hz), 7.35–7.27 (m, 2H), 7.26–7.18 (m, 2H), 7.08 (s, 2H), 5.11 (br. s, 2H), 4.98–4.88 (m, 2H), 1.77–1.64 (m, 2H), 1.58–1.46 (m, 2H), 1.45–1.16 (m, 12H); ^{13}C NMR (DMSO-d_6, 100 MHz) δ/ppm: 152.8, 135.8, 133.2, 127.7, 127.4, 125.4, 125.3, 124.9, 122.5, 108.3, 67.2, 37.8, 29.1, 29.0, 25.4; HRMS (MALDI TOF/TOF) calcd for $C_{30}H_{34}O_4$ $[M + Na]^+$ 481.2349 found 481.2332.

1,6-Bis(3-hydroxy-2-anthryl)hexane-1,6-diol (5a)

According to the general procedure from **8a** (120 mg, 0.16 mmol) the reaction furnished the product (42 mg, 50%) in the form of a beige solid.

Mp > 350 °C (decomposition); ^{1}H NMR (DMSO-d_6, 600 MHz) δ/ppm: 9.96 (br. s, 2H), 8.38 (s, 2H), 8.21 (s, 2H), 7.98 (s, 2H), 7.96 (d, 2H, J = 8.0 Hz), 7.93 (d, 2H, J = 8.4 Hz), 7.40 (t, 2H, J = 7.3 Hz), 7.35 (t, 2H, J = 7.3 Hz), 7.19 (s, 2H), 5.21–5.13 (m, 2H), 4.99–4.92 (m, 2H), 1.85–1.75 (m, 2H), 1.61–1.36 (m, 6H); ^{13}C NMR (DMSO-d_6, 150 MHz) δ/ppm: 153.0, 137.6, 131.9, 131.2, 129.4, 128.0, 127.4, 127.3, 125.5,

125.0, 124.9, 123.8, 122.2, 106.3, 67.48, 67.44, 37.8, 25.63, 25.60; HRMS (MALDI TOF/TOF) calcd for $C_{34}H_{30}O_4$ $[M - H]^-$ 501.2066 found 501.2043.

1,10-Bis(3-hydroxy-2-anthryl)decane-1,10-diol (5e)

According to the general procedure from **8e** (142 mg, 0.18 mmol) the reaction furnished the product (75 mg, 74%) in the form of a beige solid.

Mp 250–252 °C; ^{1}H NMR (DMSO-d_6, 400 MHz) δ/ppm: 9.96 (s, 2H), 8.39 (s, 2H), 8.21 (s, 2H), 7.99 (s, 2H), 7.96 (d, 2H, J = 8.4 Hz), 7.93 (d, 2H, J = 8.3 Hz), 7.43–7.31 (m, 4H), 7.20 (s, 2H), 5.21–5.14 (m, 2H), 5.00–4.91 (m, 2H), 1.83–1.71 (m, 2H), 1.59–1.47 (m, 2H), 1.48–1.33 (m, 4H), 1.33–1.17 (m, 8H); ^{13}C NMR (DMSO-d_6, 100 MHz) δ/ppm: 153.0, 137.6, 131.9, 131.2, 129.4, 128.0, 127.4, 127.3, 125.5, 125.0, 124.9, 123.8, 122.2, 106.2, 67.3, 37.7, 29.1, 29.0, 25.4; HRMS (MALDI TOF/TOF) calcd for $C_{38}H_{38}O_4$ $[M - H]^-$ 557.2692 found 557.2689.

Preparative irradiation experiments – general

A quartz vessel was filled with a solution of bis-naphthol (0.05 mmol) in CH_3OH (80 mL) and H_2O (20 mL). The solution was purged with Ar for 15 min and irradiated for 1 h in a Rayonet photochemical reactor equipped with 10 lamps with the output at 300 nm (1 lamp: 8 W). During the irradiation the solution was continuously purged with Ar and cooled with a tap-H_2O finger-condenser. The course of the reaction was followed by UPLC-MS/UV. The solvent was removed on a rotary evaporator and the residue purified using a preparative HPLC-MS/UV system.

Irradiation of 4a

According to the general procedure, after irradiation of **4a** (20 mg, 0.05 mmol) and chromatography, products **10a** (6 mg, 28%) and **11a** (15 mg, 67%) were isolated in the form of yellowish solids.

3,3′-(1-Hydroxy-6-methoxyhexane-1,6-diyl)bis(2-naphthol) (10a). A diastereoisomer mixture; mp 63–65 °C; ^{1}H NMR ($CDCl_3$, 400 MHz) δ/ppm: 7.99 (d, 1H, J = 5.5 Hz), 7.84 (br. s, 1H), 7.72–7.62 (m, 4H), 7.44–7.35 (m, 4H), 7.33–7.26 (m, 2H), 7.23–7.19 (m, 2H), 4.99–4.90 (m, 1H), 4.38 (q, 1H, J = 6.8 Hz), 3.37 (d, 3H, J = 7.6 Hz), 2.61 (br. s, 1H), 2.06–1.90 (m, 2H), 1.90–1.71 (m, 2H), 1.55–1.42 (m, 2H), 1.40–1.24 (m, 2H); ^{13}C NMR ($CDCl_3$, 125 MHz) δ/ppm: 153.5, 153.4, 134.4, 134.2, 129.7, 128.1, 127.8, 127.7, 127.5, 127.3, 126.3, 126.3, 126.2, 123.6, 111.6, 111.4, 86.0, 85.9, 76.09, 76.07, 57.3, 36.8, 36.7, 35.7, 35.6, 25.5; HRMS (MALDI TOF/TOF) calcd for $C_{27}H_{28}O_4$ $[M + Na]^+$ 439.1885, found 439.1885.

3,3′-(1,6-Dimethoxyhexane-1,6-diyl)bis(2-naphthol) (11a). Mp 48–49 °C; ^{1}H NMR ($CDCl_3$, 400 MHz) δ/ppm: 7.90–7.77 (m, 2H), 7.58–7.45 (m, 4H), 7.25–7.20 (m, H), 7.17–7.08 (m, 2H), 7.06 (s, 2H), 4.20 (q, 2H, J = 6.9 Hz), 3.22 (s, 3H), 3.20 (s, 3H), 1.90–1.74 (m, 2H), 1.66–1.53 (m, 2H), 1.36–1.24 (m, 2H), 1.19–1.07 (m, 2H); ^{13}C NMR ($CDCl_3$, 100 MHz) δ/ppm: 153.4, 134.4, 128.0, 127.79, 127.76, 127.38, 127.35, 126.3, 126.2, 123.5, 111.3, 86.0, 85.9, 57.3, 35.7, 35.6, 25.58, 25.52; HRMS (MALDI TOF/TOF) calcd for $C_{28}H_{30}O_4$ $[M + Na]^+$ 453.2042 found 453.2037.

Irradiation of 4b

According to the general procedure, after irradiation of **4b** (20 mg, 0.05 mmol) and chromatography, products **10b** (2 mg, 10%) and **11b** (9 mg, 42%) were isolated in the form of yellowish solids.

3,3′-(1-Hydroxy-7-methoxyheptane-1,7-diyl)bis(2-naphthol) (10b). A diastereoisomer mixture; mp 45–47 °C; ^{1}H NMR ($CDCl_3$, 500 MHz) δ/ppm: 8.03 (br. s, 2H), 7.73–7.63 (m, 4H), 7.46–7.34 (m, 4H), 7.32–7.26 (m, 2H), 7.23–7.17 (m, 2H), 4.97–4.87 (m, 1H), 4.39 (t, 1H, J = 7.0 Hz), 3.38 (s, 3H), 2.03–1.89 (m, 2H), 1.88–1.70 (m, 2H), 1.51–1.39 (m, 2H), 1.38–1.20 (m, 4H); ^{13}C NMR ($CDCl_3$, 125 MHz) δ/ppm: 134.2, 129.9, 128.0, 127.7, 127.5, 127.3, 126.3, 126.2, 126.1, 123.5, 111.5, 111.3, 86.1, 76.1, 57.3, 36.9, 35.7, 29.0, 15.7, 25.6; the signals of two quaternary C-atoms were not observed; HRMS (MALDI TOF/TOF) calcd for $C_{28}H_{30}O_4$ $[M + Na]^+$ 453.2042 found 453.2038.

3,3′-(1,7-Dimethoxyheptane-1,7-diyl)bis(2-naphthol) (11b). Mp 39–40 °C; ^{1}H NMR ($CDCl_3$, 500 MHz) δ/ppm: 8.01 (br. s, 2H), 7.72–7.65 (m, 4H), 7.45–7.35 (m, 4H), 7.32–7.26 (m, 2H), 7.22 (s, 2H), 4.38 (t, 2H, J = 6.8 Hz), 3.39 (s, 3H), 3.38 (s, 3H), 2.05–1.91 (m, 2H), 1.80–1.69 (m, 2H), 1.49–1.37 (m, 2H), 1.36–1.18 (m, 4H); ^{13}C NMR ($CDCl_3$, 125 MHz) δ/ppm: 153.5, 134.4, 128.1, 127.8, 127.5, 127.3, 126.3, 123.5, 111.3, 86.1, 57.3, 35.8, 29.1, 25.7; HRMS (MALDI TOF/TOF) calcd for $C_{29}H_{32}O_4$ $[M + Na]^+$ 467.2198 found 467.2201.

Irradiation of 4e

According to the general procedure, after irradiation of **4e** (20 mg, 0.04 mmol) and chromatography, products **10e** (3 mg, 13%) and **11e** (8 mg, 38%) were isolated in the form of yellowish solids.

3,3′-(1-Hydroxy-10-methoxydecane-1,10-diyl)bis(2-naphthol) (10e). A diastereoisomer mixture; mp 44–45 °C; ^{1}H NMR ($CDCl_3$, 500 MHz) δ/ppm: 8.06 (s, 1H), 7.94 (br. s, 1H), 7.73–7.64 (m, 4H), 7.47–7.42 (m, 2H), 7.42–7.36 (m, 2H), 7.32–7.27 (m, 2H), 7.23 (s, 2H), 4.98 (t, 1H, J = 6.6 Hz), 4.41 (t, 1H, J = 7.0 Hz), 3.40 (s, 3H), 2.63 (br. s, 1H), 2.04–1.90 (m, 2H), 1.89–1.79 (m, 1H), 1.79–1.72 (m, 1H), 1.50–1.35 (m, 2H), 1.34–1.14 (m, 10H); ^{13}C NMR ($CDCl_3$, 125 MHz) δ/ppm: 129.7, 128.1, 127.8, 127.5, 127.3, 126.34, 126.30, 126.2, 123.58, 123.53, 111.6, 111.3, 86.3, 76.4, 57.3, 37.0, 35.8, 29.2, 25.7, the signals of two quaternary C-atoms and two tertiary C-atoms were not observed; HRMS (MALDI TOF/TOF) calcd for $C_{31}H_{36}O_4$ $[M + Na]^+$ 495.2511 found 495.2509.

3,3′-(1,10-Dimethoxydecane-1,10-diyl)bis(2-naphthol) (11e). Mp 32–35 °C; ^{1}H NMR ($CDCl_3$, 500 MHz) δ/ppm: 8.09 (s, 2H), 7.74 (t, 4H, J = 8.7 Hz), 7.49 (s, 2H), 7.45 (t, 2H, J = 7.4 Hz), 7.34 (t, 2H, J = 7.4 Hz), 7.27 (s, 2H), 4.44 (t, 2H, J = 7.2 Hz), 3.44 (s, 6H), 2.08–1.94 (m, 2H), 1.86–1.74 (m, 2H), 1.53–1.39 (m, 2H), 1.37–1.19 (m, 10H); ^{13}C NMR ($CDCl_3$, 125 MHz) δ/ppm: 153.6, 134.4, 128.1, 127.8, 127.6, 127.4, 126.3, 123.5, 111.3, 86.3, 57.3, 35.9, 29.3, 29.2, 25.8; HRMS (MALDI TOF/TOF) calcd for $C_{32}H_{38}O_4$ $[M + Na]^+$ 509.2668 found 509.2678.

Preparation of 3,3′-(1,10-dimethoxydecane-1,10-diyl) bis(2-anthrol) (12e)

A flask (50 mL) was charged with **5e** (18 mg, 0.03 mmol) and methanol (20 mL). To the suspension concentrated sulfuric acid (w = 98%, 0.1 mL) was added. After 16 h of stirring at rt, the reaction mixture was diluted with water (20 mL) and carefully neutralized with saturated aqueous $NaHCO_3$ solution (≈4 mL). The mixture was transferred to a separation funnel, and extracted with ethyl acetate (3 × 15 mL). The organic extracts were dried over anhydrous $MgSO_4$ and filtered, and the solvent was removed on a rotary evaporator. The pure product **12e** (8 mg, 43%) was isolated by preparative HPLC-MS/UV in the form of a beige solid.

Mp 65–68 °C; ^{1}H NMR ($CDCl_3$, 600 MHz) δ/ppm: 8.29 (s, 2H), 8.23 (s, 2H), 8.09 (s, 2H), 7.96–7.90 (m, 4H), 7.62 (s, 2H), 7.44–7.36 (m, 4H), 7.34 (s, 2H), 4.44 (t, 2H, J = 7.2 Hz), 3.43 (s, 3H), 3.43 (s, 3H), 2.07–1.96 (m, 2H), 1.84–1.75 (m, 2H), 1.48–1.39 (m, 2H), 1.31–1.21 (m, 10H); ^{13}C NMR ($CDCl_3$, 150 MHz) δ/ppm: 153.1, 132.5, 132.2, 130.3, 129.0, 128.1, 128.0, 127.6, 127.4, 125.9, 125.4, 124.4, 123.6, 109.6, 86.4, 57.3, 35.8, 29.3, 29.2, 25.9.

Quantum yield of photomethanolysis

The quantum yield of the photomethanolysis reaction was determined by using KI/KIO_3 (Φ_{254} = 0.74)[44,45] as an actinometer. The solutions of compounds **4** in CH_3OH–H_2O (4 : 1) were prepared in concentrations corresponding to absorbances in the range 0.5–0.9 at 254 nm. The solutions were purged with an Ar stream (15 min each) and then sealed with a cap. The solutions of compounds and the actinometer were irradiated in quartz cuvettes, at the same time with one lamp (254 nm, 8 W). Yields on products **10**, formed from **4**, were determined by UPLC-MS/UV and the obtained values were used for the calculation of quantum yields (eqn (S6) in the ESI†). Measurements were carried out three times in three independent experiments, and the average value is reported.

Photochemical alkylation of BSA and HSA with 4a

A solution (2 mL) containing **4a** (c = 5.60 × 10^{-5} M) and BSA (c = 1.20 × 10^{-4} M) or HSA (c = 1.42 × 10^{-4} M) in aqueous sodium phosphate buffer (c = 0.05 M, pH 0 7.0) : CH_3CN 1 : 1 was irradiated in a Luzchem reactor (8 lamps, 350 nm, 1 lamp: 8 W) for 10 min. The irradiated solution was diluted in CH_3CN and 0.05 M phosphate buffer (1 : 1; v/v) at a concentration of 10^{-4} M and analyzed by MALDI-TOF mass spectrometry. Prior to the analysis, 100 μL of the irradiated solution was purified using Aspire RP30 Desalting Tips (Thermo Fisher Scientific, MA, USA). After the purification, the solvent was evaporated in a Speed-Vac (Eppendorf, Switzerland) and re-constituted in 10 μL of the sinapinic acid matrix (5 mg mL^{-1} of sinapinic acid in 1 : 1, CH_3CN : 0.1% TFA, v/v). The mixture of the analyte and the matrix was deposited onto the MALDI plate (1 μL) and dried slowly in a stream of cold air. MALDI mass spectra were recorded on an AB SCIEX MALDI-TOF/TOF 4800+ (MA, USA). It was operated in linear ion mode with the following parameters: delay time: 1500 ns, laser power: 4550 and mass range: 20 000–150 000 Da, with a 66 600 mass center. Applied calibration was external, performed with AB SCIEX BSA and an IgG1 mass standard kit. Minimum ten spectra were averaged to obtain the average molecular mass (see Tables S1 and S2 in the ESI†).

Absorption and fluorescence measurements

UV-Vis spectra were recorded on a Varian Cary 100 Bio spectrophotometer at rt. Fluorescence measurements were performed on an Agilent Cary Eclipse fluorometer by using slits corresponding to a bandpass of 2.5 nm for the excitation and 5.0 nm for the emission. Fluorescence quantum yields were determined by using quinine sulfate in 1.0 N H_2SO_4 (Φ_f = 0.546) as a reference.[32] One fluorescence measurement was performed by exciting the sample at three different wavelengths (300, 310 and 320 nm), and the average value was calculated (see eqn (S1)–(S5) in the ESI†). Prior to the measurements, the solutions were purged with Ar for 15 min. The measurement was performed at rt (25 °C).

For the investigation of noncovalent binding to BSA and HSA, stock solutions of bis-naphthol **4a** in CH_3CN (c = 7.45 × 10^{-4} M), and BSA (c = 5.71 × 10^{-4} M) or HSA (c = 5.80 × 10^{-4} M) in sodium phosphate buffer (pH = 7.0, c = 0.05 M) were prepared, which were further diluted. The titrations were performed by adding aliquots of the protein stock solution to the solution of **4a** (c = 1.49 × 10^{-5} M) in aqueous sodium phosphate buffer (pH = 7.0, c = 0.05 M) : CH_3CN = 1 : 1. The sample was excited at 320 nm, and the fluorescence spectra were recorded by using slits corresponding to the band pass of 5 nm.

Single photon counting

The SPC set-up consisted of a PicoQuant (Berlin, Germany) PLS 267 nm pulsed LED with a repetition rate of 10 MHz and a Becker&Hickl (Berlin, Germany) SPC630 MCA card was applied. The detector, an R5600A-U04 from Hamamatsu (Herrsching, Germany), was used with a HP 6110A power supply from HP at 900 V and an amplifier HF02 (+20 dB, 2 × 5828A, 70 kHz to 14 GHz from PicoSecond Pulse Labs, Boulder, CO, USA), together with a 6.5 GHz power limiter HTZ, 93346 MIC3171-1 (AEL *via* C. Plath GmbH, Hamburg, Germany). To reduce the dark signal the detector was cooled with a Peltier Cooler Model 350 (Light Control Instruments Inc.) to 15 °C. The IRF of this set-up is 250 ps. The fluorescence signal was separated with different band-pass filters to assure almost monochromatic detection. The time traces (4096 channels) were analyzed by the PicoQuant FluoFit (Version 4.6.6) software and fit to eqn (S7) in the ESI.†

Laser flash photolysis

The measurements were performed on a LP980 Edinburgh Instruments spectrometer. For the excitation the fourth harmonic of a Qsmart Q450 Quantel YAG laser was used. The energy of the laser pulse at 266 nm was set to 20 mJ and the pulse duration was 7 ns. Absorbances at the excitation wave-

length were set to 0.3–0.4. The static cells were used and they were frequently exchanged to ensure no absorption of light by the photoproducts. The solutions were purged for 15 min with Ar or O_2 prior to the measurements.

Conflicts of interest

There are no conflicts to declare.

Acknowledgements

These materials are based on work financed by the Croatian Science Foundation (HRZZ grant no. HRZZ IP-2014-09-6312 to NB and IP-2013-5660 to MK). The authors thank EPA Austria for support for the SPC measurements and acknowledge generous support from Fidelta Ltd.

Notes and references

1 *Quinone Methides*, ed. S. E. Rokita, Wiley, Hoboken, USA, 2009.
2 M. Freccero, Quinone Methides as Alkylating and Cross-Linking Agents, *Mini-Rev. Org. Chem.*, 2004, **1**, 403–415.
3 P. Wang, Y. Song, L. Zhang, H. He and X. Zhou, Quinone Methide derivatives: Important Intermediates to DNA Alkylating and DNA Cross-linking Actions, *Curr. Med. Chem.*, 2005, **12**, 2893–2913.
4 R. Van De Water and T. R. R. Pettus, *o*-Quinone methides: intermediates underdeveloped and underutilized in organic synthesis, *Tetrahedron*, 2002, **58**, 5367–5405.
5 T. P. Pathak and M. S. Sigman, Applications of *ortho*-Quinone Methide Intermediates in Catalysis and Asymmetric Synthesis, *J. Org. Chem.*, 2011, **76**, 9210–9215.
6 M. S. Singh, A. Nagaraju, N. Anand and S. Chowdhury, ortho-Quinone methide (o-QM): a highly reactive, ephemeral and versatile intermediate in organic synthesis, *RSC Adv.*, 2014, **4**, 55924–55959.
7 W. J. Bai, J. G. David, Z.-G. Feng, M. G. Weaver, K.-L. Wu and T. R. R. Pettus, The Domestication of ortho-Quinone Methides, *Acc. Chem. Res.*, 2014, **47**, 3655–3664.
8 A. A. Jaworski and A. K. Scheidt, Emerging Roles of in Situ Generated Quinone Methides in Metal-Free Catalysis, *J. Org. Chem.*, 2016, **81**, 10145–10153.
9 E. Modica, R. Zanaletti, M. Freccero and M. Mella, Alkylation of Amino Acids and Glutathione in Water by *o*-Quinone Methide. Reactivity and Selectivity, *J. Org. Chem.*, 2001, **66**, 41–52.
10 S. Arumugam, J. Guo, N. E. Mbua, F. Fiscourt, N. Lin, E. Nekongo, G. J. Boons and V. V. Popik, Selective and Reversible Photochemical Derivatization of Cysteine Residues in Peptides and Proteins, *Chem. Sci.*, 2014, **5**, 1591–1598.
11 S. E. Rokita, J. Yang, P. Pande and W. A. Greenberg, Quinone Methide Alkylation of Deoxycytidine, *J. Org. Chem.*, 1997, **62**, 3010–3012.
12 W. F. Veldhuyzen, A. J. Shallop, R. A. Jones and S. E. Rokita, Thermodynamic versus Kinetic Products of DNA Alkylation as Modeled by Reaction of Deoxyadenosine, *J. Am. Chem. Soc.*, 2001, **123**, 11126–11132.
13 E. E. Weinert, K. N. Frankenfield and S. E. Rokita, Time-Dependent Evolution of Adducts Formed Between Deoxynucleosides and a Model Quinone Methide, *Chem. Res. Toxicol.*, 2005, **18**, 1364–1370.
14 E. E. Weinert, D. Ruggero, S. Colloredo-Melz, K. N. Frankenfield, C. H. Mitchell, M. Freccero and S. E. Rokita, Substituents on Quinone Methides Strongly Modulate Formation and Stability of their Nucleophilic Adducts, *J. Am. Chem. Soc.*, 2006, **128**, 11940–11947.
15 M. Chatterjee and S. E. Rokita, The Role of a Quinone Methide in the Sequence Specific Alkylation of DNA, *J. Am. Chem. Soc.*, 1994, **116**, 1690–1697.
16 Q. Zeng and S. E. Rokita, Tandem Quinone Methide Generation for Cross-Linking DNA, *J. Org. Chem.*, 1996, **61**, 9080–9081.
17 P. Pande, J. Shearer, J. Yang, W. A. Greenberg and S. E. Rokita, Alkylation of Nucleic Acids by a Model Quinone Methide, *J. Am. Chem. Soc.*, 1999, **121**, 6773–6779.
18 D. Verga, M. Nadai, F. Doria, C. Percivalle, M. Di Antonio, M. Palumbo, S. N. Richter and M. Freccero, Photogeneration and Reactivity of Naphthoquinone Methides as Purine Selective DNA Alkylating Agents, *J. Am. Chem. Soc.*, 2010, **132**, 14625–14637.
19 M. Nadai, F. Doria, M. Di Antonio, G. Sattin, L. Germani, C. Percivalle, M. Palumbo, S. N. Richter and M. Freccero, Naphthalene diimide scaffolds with dual reversible and covalent interaction properties towards G-quadruplex, *Biochemie*, 2011, **93**, 1328–1340.
20 F. Doria, M. Nadai, M. Folini, M. Di Antonio, L. Germani, C. Percivalle, C. Sissi, N. Zaffaroni, S. Alcaro, A. Artese, S. N. Richter and M. Freccero, Hybrid ligand–alkylating agents targeting telomeric G-quadruplex structures, *Org. Biomol. Chem.*, 2012, **10**, 2798–2806.
21 F. Doria, M. Nadai, M. Folini, M. Scalabrin, L. Germani, G. Sattin, M. Mella, M. Palumbo, N. Zaffaroni, D. Fabris, M. Freccero and S. N. Richter, Targeting Loop Adenines in G-Quadruplex by a Selective Oxirane, *Chem. – Eur. J.*, 2013, **19**, 78–81.
22 H. Wang, M. S. Wahi and S. E. Rokita, Immortalizing a Transient Electrophile for DNA Cross-Linking, *Angew. Chem., Int. Ed.*, 2008, **47**, 1291–1293.
23 H. Wang, S. E. Rokita and S. E. Dynamic, Cross-Linking is Retained in Duplex DNA after Multiple Exchange of Strands, *Angew. Chem., Int. Ed.*, 2010, **49**, 5957–5960.
24 C. S. Rossiter, E. Modica, D. Kumar and S. E. Rokita, Few constraints limit the design of quinone methide-oligonucleotide self-adducts for directing DNA alkylation, *Chem. Commun.*, 2011, **47**, 1476–1478.

25 F. Fakhari and S. E. Rokita, A walk along DNA using bipedal migration of a dynamic and covalent crosslinker, *Nat. Commun.*, 2014, **5**, 5591, DOI: 10.1038/ncomms6591.

26 V. S. Li and H. Kohn, Studies on the Bonding Specificity for Mitomycin C-DNA Monoalkylation Processes, *J. Am. Chem. Soc.*, 1991, **113**, 275–283.

27 I. Han, D. J. Russell and H. Kohn, Studies on the Mechanism of Mitomycin C(1) Electrophilic Transformations: Structure-Reactivity Relationships, *J. Org. Chem.*, 1992, **57**, 1799–1807.

28 M. Tomasz, A. Das, K. S. Tang, M. G. J. Ford, A. Minnock, S. M. Musser and M. J. Waring, The Purine 2-Amino Group as the Critical Recognition Element for Sequence-Specific Alkylation and Cross-Linking of DNA by Mitomycin C, *J. Am. Chem. Soc.*, 1998, **120**, 11581–11593.

29 N. Basarić, K. Mlinarić-Majerski and M. Kralj, Quinone Methides: Photochemical Generation and its Application in Biomedicine, *Curr. Org. Chem.*, 2014, **18**, 3–18.

30 C. Percivalle, F. Doria and M. Freccero, Quinone Methides as DNA Alkylating Agents: An Overview on Efficient Activation Protocols for Enhanced Target Selectivity, *Curr. Org. Chem.*, 2014, **18**, 19–43.

31 K. Nakatani, N. Higashida and I. Saito, Highly Efficient Photochemical Generation of o-Quinone Methide from Mannich Bases of Phenol Derivatives, *Tetrahedron Lett.*, 1997, **38**, 5005–5008.

32 Đ. Škalamera, C. Bohne, S. Landgraf and N. Basarić, Photodeamination reaction mechanism in aminomethyl *p*-cresol derivatives: different reactivity of amines and ammonium salts, *J. Org. Chem.*, 2015, **80**, 10817–10828.

33 L. Diao, C. Yang and P. Wan, Quinone Methide Intermediates from the Photolysis of Hydroxybenzyl Alcohols in Aqueous Solution., *J. Am. Chem. Soc.*, 1995, **117**, 5369–5370.

34 Đ. Škalamera, I. Antol, K. Mlinarić-Majerski, H. Vančik, D. L. Phillips, J. Ma and N. Basarić, Ultrafast Adiabatic Photodehydration of 2-Hydroxymethylphenol and the Formation of Quinone Methide, *Chem. – Eur. J.*, 2018, **24**, 9426–9435.

35 N. Basarić, N. Cindro, D. Bobinac, K. Mlinarić-Majerski, L. Uzelac, M. Kralj and P. Wan, Sterically Congested Quinone Methides in Photodehydration Reactions of 4-Hydroxybiphenyl Derivatives and Investigation of their Antiproliferative Activity, *Photochem. Photobiol. Sci.*, 2011, **10**, 1910–1925.

36 N. Basarić, N. Cindro, D. Bobinac, L. Uzelac, K. Mlinarić-Majerski, M. Kralj and P. Wan, Zwitterionic Biphenyl Quinone Methides in Photodehydration Reactions of 3-Hydroxybiphenyl Derivatives: Laser Flash Photolysis and Antiproliferation Study, *Photochem. Photobiol. Sci.*, 2012, **11**, 381–396.

37 J. Veljković, L. Uzelac, K. Molčanov, K. Mlinarić-Majerski, M. Kralj, P. Wan and N. Basarić, Sterically Congested Adamantylnaphthalene Quinone Methides, *J. Org. Chem.*, 2012, **77**, 4596–4610.

38 Đ. Škalamera, K. Mlinarić-Majerski, I. Martin Kleiner, M. Kralj, J. Oake, P. Wan, C. Bohne and N. Basarić, Photochemical Formation of Anthracene Quinone Methide Derivatives, *J. Org. Chem.*, 2017, **82**, 6006–6021.

39 L. Uzelac, Đ. Škalamera, K. Mlinarić-Majerski, N. Basarić and M. Kralj, Selective photocytotoxicity of anthrols on cancer stem-like cells: The effect of quinone methides or reactive oxygen species, *Eur. J. Med. Chem.*, 2017, **137**, 558–574.

40 M. Sambol, K. Ester, A. Husak, Đ. Škalamera, I. Piantanida, M. Kralj and N. Basarić, Bifunctional Phenol Quinone Methide Precursors: Synthesis and Biological Activity, *Croat. Chem. Acta*, DOI: 10.5562/cca3455.

41 S. R. Rajski and R. M. Williams, DNA Cross-Linking Agents as Antitumor Drugs, *Chem. Rev.*, 1998, **98**, 2723–2725.

42 S. Arumugam and V. V. Popik, Photochemical Generation and the Reactivity of *o*-Naphthoquinone Methides in Aqueous Solutions, *J. Am. Chem. Soc.*, 2009, **131**, 11892–11899.

43 V. Markovic, D. Villamaina, I. Barbanov, L. M. Lawson Daku and E. Vauthey, Photoinduced Symmetry-Breaking Charge Separation: The Direction of the Charge Transfer, *Angew. Chem., Int. Ed.*, 2011, **50**, 7596–7598.

44 M. Montalti, A. Credi, L. Prodi and M. T. Gandolfi, in *Handbook of Photochemistry*, CRC Taylor and Francis, Boca Raton, 2006.

45 S. Goldstein and J. Rabani, The ferrioxalate and iodide-iodate actinometers in the UV region, *J. Photochem. Photobiol., A*, 2008, **193**, 50–55.

46 W. R. Laws and L. Brand, Analysis of Two-State Excited-State Reactions. The Fluorescence Decay of 2-Naphthol, *J. Phys. Chem.*, 1979, **83**, 795–802.

47 J. Lee, G. W. Robinson, S. P. Webb, L. A. Philips and J. H. Clark, Hydration dynamics of protons from photon initiated acids, *J. Am. Chem. Soc.*, 1986, **108**, 6538–6542.

48 G. W. Robinson, Proton charge transfer involving the water solvent, *J. Phys. Chem.*, 1991, **95**, 10386–10391.

49 L. M. Tolbert and J. E. Haubrich, Photoexcited proton transfer from enhanced photoacids, *J. Am. Chem. Soc.*, 1994, **116**, 10593–10600.

50 K. M. Solntsev, D. Huppert, N. Agmon and L. M. Tolbert, Photochemistry of "super" photoacids. 2. Excited-state proton transfer in methanol/water mixtures, *J. Phys. Chem. A*, 2000, **104**, 4658–4669.

51 L. M. Tolbert and K. M. Solntsev, Excited-State Proton Transfer: From Constrained Systems to "Super" Photoacids to Superfast Proton Transfer, *Acc. Chem. Res.*, 2002, **35**, 19–27.

52 A. M. Brouwer, Standards for photoluminescence quantum yield measurements in solution (IUPAC Technical Report), *Pure Appl. Chem.*, 2011, **83**, 2213–2228.

53 J. F. Ireland and P. A. H. Wyatt, Acid-Base Properties of Electronically Excited States of Organic Molecules, *Adv. Phys. Org. Chem.*, 1976, **12**, 131–221.

54 A. Liu, M. C. Sauer, Jr., D. M. Loffredo and A. D. Trifunac, Transient Absorption Spectra of Aromatic Radical Cations in Hydrocarbon Solutions, *J. Photochem. Photobiol., A*, 1992, **67**, 197–208.

55 C. Kerzig and M. Goez, Highly Efficient Green-Light Ionization of an Aryl Radical Anion: Key Step in a Catalytic Cycle of Electron Formation, *Phys. Chem. Chem. Phys.*, 2014, **16**, 25342–25349.
56 E. Vauthey, E. Haselbach and P. Suppan, Photoionization of Naphthalene and Anthracene in Acetonitrile, *Helv. Chim. Acta*, 1987, **70**, 347–353.
57 T. Shida and S. Iwata, Electronic Spectra of Ion Radicals and Their Molecular Orbital Interpretation. 111. Aromatic Hydrocarbons, *J. Am. Chem. Soc.*, 1973, **95**, 3473–3783.
58 L. Pretali, F. Doria, D. Verga, A. Profumo and M. Freccero, Photoarylation/Alkylation of Bromonaphthols, *J. Org. Chem.*, 2009, **74**, 1034–1041.
59 T. A. Gadosy, D. Shukla and L. J. Johnston, Generation, Characterization, and Deprotonation of Phenol Radical Cations, *J. Phys. Chem. A*, 1999, **103**, 8834–8839.
60 Y. Chiang, A. J. Kresge and Y. Zhu, Kinetics and Mechanisms of Hydration of *o*-Quinone Methides in Aqueous Solution, *J. Am. Chem. Soc.*, 2000, **122**, 9854–9855.
61 I. Vaya, V. Lhiaubert-Vallet, M. Consuelo Jiménez and M. A. Miranda, Photoactive assemblies of organic compounds and biomolecules: drug-protein supramolecular systems, *Chem. Soc. Rev.*, 2014, **43**, 4102–4122.
62 R. Pérez-Ruiz, O. Molins-Molina, E. Lence, C. González-Bello, M. A. Miranda and M. Consuelo Jiménez, Photogeneration of Quinone Methides as Latent Electrophiles for Lysine Targeting, *J. Org. Chem.*, 2018, **83**, 13019–13029.
63 E. Ahmad, G. Rabbani, N. Zaidi, S. Singh, M. Rehan, M. M. Khan, S. K. Rahman, Z. Quadri, M. Shadab, M. T. Ashraf, N. Subbarao, R. Bhat and R. H. Khan, Stereo-Selectivity of Human Serum Albumin to Enantiomeric and Isoelectronic Pollutants Dissected by Spectroscopy, Calorimetry and Bioinformatics, *PLoS One*, 2011, **6**, e26186 1–e2618618.
64 A. Gajahi Soudahome, A. Catan, P. Giraud, S. Assouan Kouao, A. Guerin-Dubourg, X. Debussche, N. Le Moullec, E. Bourdon, S. B. Bravo, B. Paradela-Dobarro, E. Álvarez, O. Meilha, P. Rondeau and J. Couprie, Glycation of human serum albumin impairs binding to the glucagon-like peptide-1 analogue liraglutide, *J. Biol. Chem.*, 2018, **293**, 4778–4791.